Refining Interpretation of MIBG Scans in Children

François Bonnin, Jean Lumbroso, Florence Tenenbaum, Olivier Hartmann and Claude Parmentier

Department of Nuclear Medicine and Department of Pediatric Oncology, Institut Gustave-Roussy, Villejuif France

In pediatrics, the distribution of radioiodinated metaiodobenzyl-guanidine (MIBG) has been studied primarily in neuroblastoma. However, normal patterns in children show a number of particularities and pitfalls related to the context of pediatric oncology which must be identified. **Methods:** We report on 28 equivocal scans in 24 children. In all cases, two experienced observers judged the scans to be equivocal and the definite interpretations were confirmed by follow-up. **Results:** Difficulties in interpreting the scans were observed at the level of the thorax (15 patients), the abdomen (5 patients), the head (4 patients) or elsewhere (4 patients). The final interpretation of the scans was attributed to an unusual physiological pattern linked to age (9 patients), tumoral context (17 patients) or artifacts (2 patients). **Conclusions:** A number of important physiological areas of uptake in soft tissues can lead to false-positive interpretations of normal scans, such as the physiological upper thoracic uptake which has never been previously described. Numerous technical and physiological possibilities exist and those pitfalls must be ruled out. A precise knowledge of these technical difficulties and physiological variants can reduce the number of equivocal MIBG scans.

Key Words: pediatrics; neuroblastoma; metaiodobenzylguanidine

J Nucl Med 1994; 35:803–810

O ne decade after its clinical introduction, radioiodinated metaiodobenzylguanidine (MIBG) (*1*) has established its place in the diagnosis of tumors derived from the neural crest. In adults, the normal distribution of radioiodinated MIBG (*2*) has been well described (*3,4*). In children, pathological distributions of MIBG labeled with [131]I-(*5–9*) or with [123]I (*10,11*) have been studied, especially in neuroblastoma. However, normal patterns of MIBG biodistribution in children show particularities which render interpretation difficult. Moreover, pitfalls related to the context of pediatric oncology must be recognized to avoid misinterpretations. The aim of this paper is to illustrate how a precise interpretative analysis of MIBG scans can improve the use of this technique.

PATIENTS AND METHODS

Patients

Twenty-eight equivocal scans were obtained from 24 children (Table 1). The median age at diagnosis was 8 mo (range: newborn to 10 yr). Patient 24 was subsequently found to be free of tumor; 23 children (11 boys and 12 girls) suffered from neuroblastoma. Diagnosis of neuroblastoma was based on either histology or bone marrow cytological findings in patients with elevated urinary excretion of catecholamines and/or catecholamine metabolites (vanillylmandelic acid, homovanillic acid, dopamine). In the group of children with neuroblastoma, 12 were less than 1 yr old.

All scans were obtained with ^{123}I-MIBG. The labeling of MIBG was done according to the method of Manger (*2*) using a kit for ^{123}I supplied by CIS Bio International (Gif-sur-Yvette, France).

TABLE 1
Description of the 24 Children with Equivocal Scans

Patient no.	Sex/age at diagnosis	Diagnosis/ Stage*	Primary tumor site	Hormonal urinary excretion
1	F/6 mo	NB/IVs	Right adrenal	Elevated
2	F/4 mo	NB/IVs	Not found	Elevated
3	F/2 mo	NB/IVs	Left adrenal	Elevated
4	F/5 mo	NB/IVs	Not found	Elevated
5	M/4 mo	NB/IVs	Not found	Elevated
6	M/10 mo	NB/IV	Left adrenal	Elevated
7	M/14 mo	NB/IV	Right adrenal	Elevated
8	M/5 yr	NB/IV	Abdominal	Elevated
9	F/2.5 yr	NB/IV	Abdominal	Elevated
10	F/4.5 yr	NB/IV	Abdominal	Elevated
11	M/2 yr	NB/IV	Abdominal	Elevated
12	F/7 yr	NB/IV	Right adrenal	Elevated
13	M/3.5 yr	NB/IV	Abdominal	Elevated
14	M/4 yr	NB/IV	Right adrenal	Elevated
15	F/10 yr	NB/IV	Abdominal	Elevated
16	M/4 mo	NB/III	Thorax	Elevated
17	F/2 yr	NB/III	Right adrenal	Elevated
18	M/newborn	NB/III	Cervical	Normal
19	F/8 mo	NB/III	Abdominal/Pelvic	Elevated
20	F/7 yr	NB/III	Right adrenal	Elevated
21	M/newborn	NB/II	Abdominal	Elevated
22	M/7 mo	NB/II	Left adrenal	Elevated
23	F/1.5 mo	NB/I	Thorax	Normal
24	M/8 mo	Normal	None	Normal

*TNM classification.
NB = neuroblastoma.

TABLE 2
Description of Equivocal Scans

Patient no.	Site	Type of problem	Context	Origin	Validated by
Normal patterns					
6	Abdomen	Intense gut uptake	Follow-up	Physiological uptake	Follow-up
12	Thorax	Unusual pleural uptake	Follow-up	Physiological uptake	Follow-up
	Head	Unique mandibulary uptake	Follow-up	Salivary excretion	Same region imaged later
13	Thorax	Irregular cardiac shape	Initial diagnosis	Physiological uptake	Follow-up
14	Head	Unique mandibulary uptake	Initial diagnosis	Physiological uptake	Follow-up
16	Thorax	Upper and bilateral uptake	Initial diagnosis	Physiological uptake	Follow-up
19	Thorax	Upper and bilateral uptake	Initial diagnosis	Physiological uptake	Follow-up
21	Thorax	Upper and bilateral uptake	Initial diagnosis	Physiological uptake	Follow-up
23	Thorax	Upper and bilateral uptake	Initial diagnosis	Physiological uptake	Follow-up
24	Thorax	Hyperintense cardiac uptake	Initial diagnosis	Physiological uptake (related to age)	Follow-up
Pitfalls and unusual pattern related to the tumoral context					
1	Thorax	Irregular cardiac shape	Follow-up	Retrocardiac costal metastasis	Radiology (CT)
	Thorax	High pulmonary uptake	Follow-up	Pulmonary metastases	Radiology (CT)
2	Head	Irregular nasal uptake	Follow-up	Occipital metastasis	Histology
3	Cutaneous	Sites not localized	Initial diagnosis	Multiple subcutaneous metastases	Follow-up (?)
5	Abdomen	Hepatic versus splenic uptake	Initial diagnosis	Tumoral left liver	Radiology (US)
7	Abdomen	Hepatic versus splenic uptake	Initial diagnosis	Necrotic liver metastasis	Radiology (US, CT)
	Thorax	Upper but unilateral uptake	Initial diagnosis	Supraclavicular lymph node metastasis	Radiology (CT)
8	Thorax	Irregular cardiac shape	Follow-up	Retrocardiac bony metastasis	Radiology (CT)
	Pelvis	Irregular bladder shape	Follow-up	Tumoral lymph node	Follow-up
10	Thorax	Irregular cardiac shape	Follow-up	Sternal metastasis	Follow-up
11	Limbs	Normal appearance of a painful leg	Follow-up	Photopenic bony metastasis	Bone scintigraphy (^{99m}Tc-HMDP)
15	Thorax	Photopenic heart	Initial diagnosis	Presence of tumoral sites	Follow-up
17	Abdomen	Digestive versus vertebral uptake	Postsurgery	Residual lymph node	Radiology (CT)
18	Head	Hemicranial photopenic aspect	Postradiotherapy	Radiotherapy and surgery	Context
20	Abdomen	Hepatic versus adrenal uptake	Initial diagnosis	Right adrenal neuroblastoma	Scintigraphy with ^{99m}Tc-colloid
22	Thorax	Photopenic heart	Initial diagnosis	Presence of tumoral sites	Follow-up
Artifacts					
4	Limbs	Pseudo-bony uptake	Initial diagnosis	Artifact of injection	Follow-up
9	Thorax	Irregular cardiac shape	Postsurgery	Artifact of injection (central line)	Lateral view

US = ultrasonography and CT = computerized tomography.
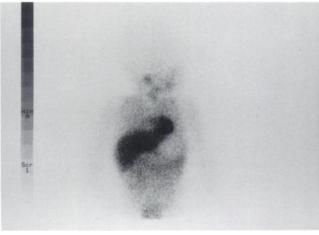

FIGURE 1. A normal pattern of MIBG distribution in a 1-yr-old boy (anterior view).

Acquisition Procedure

Iodine-123-MIBG (3.7 MBq/kg) was intravenously injected in all patients.

In order to prevent thyroid uptake of the radioiodinated tracer, Lugol's solution was administered 3 days before and 3 days after the injection of MIBG. No colonic preparation was systematically performed. All scans were performed 24 hr after the intravenous injection of ^{123}I-MIBG using a large field of view gamma camera fitted with a low-energy, all-purpose parallel-hole collimator interfaced to a dedicated computer. In all cases, anterior and posterior whole-body scans (or equivalent 256 × 256 spot images) and four cranial views were recorded. Acquisition time was 10 min per view for spot images (in the case of whole-body scans, the scanning speed was 5 cm/min) leading to a total of 40–60 min for each scan.

The staff was specifically trained to deal with pediatric patients. Time was allotted to prepare the child and his parents in a prescan
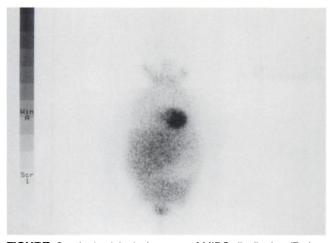
FIGURE 2. A physiological pattern of MIBG distribution (Patient 24). Hyperintense myocardial uptake in a 6-mo-old boy (anterior view).
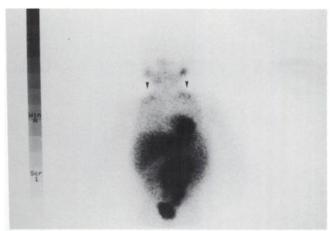

FIGURE 4. A physiological variant pattern of MIBG uptake (Patient 19). Bilateral upper thoracic uptake in a patient at diagnosis of stage-III neuroblastoma. The primary tumor site shows a very high abdominopelvic uptake (anterior view).

meeting in order to develop the child's confidence. During acquisition, attention was paid to potential urinary contamination of the child's skin. In addition, the help of a family member was always requested in order to minimize the child's movements. Younger patients (<1 yr) were immobilized using a deflatable air mattress. None of the children required premedication.
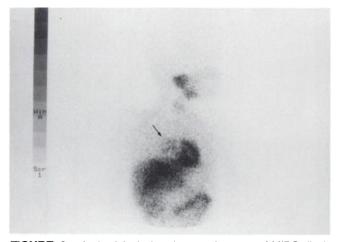
Interpretation of the Scans

In all cases, two experienced observers (FB, JL) judged the scan to be equivocal and the definite interpretations were confirmed on follow-up. The median duration of the follow-up after the equivocal scan was 1.4 yr (range: 1–4 yr). In six patients, the final diagnosis was also obtained by radiology and in one patient by histology (Table 2). In two patients (Patients 11 and 20), the equivocal image required an immediate injection of a second radiopharmaceutical (^{99m}Tc-HMDP and ^{99m}Tc-colloid, respectively). In one patient (Patient 6), later MIBG images (48 hr postinjection) were recorded.

Normal ^{123}I-MIBG Pattern in Children

The normal distribution of ^{123}I-MIBG shows myocardium and skeletal muscles, lungs, salivary glands, nasal mucosa (probably due to adrenergic innervation), liver, adrenal glands and urinary tract (probably due to excretion of MIBG).

The left ventricular uptake is usually intense at the heart level. The "right heart" uptake is more diffuse and less intense than that of the left ventricle with fuzzy edges and a slightly heterogeneous aspect, creating a paramedian mediastinal area of uptake. This uptake may correspond to atrial or nodal tracer uptake, possibly at the sinoatrial node level. Physiological pulmonary uptake is diffuse, symmetrical and low. No bony uptake is detectable on a normal scan. The physiological pattern of tracer distribution in the abdomen includes multiple physiological sites of uptake such as intense homogeneous liver uptake, gastric uptake, colonic imaging and urinary imaging. The physiological uptake by the adrenal glands is moderate and symmetrical. The normal nasal mucosal uptake is moderate and symmetrical. A thyroid image, usually

FIGURE 3. A physiological and unusual pattern of MIBG distribution (Patient 13). A particularly heterogeneous aspect of the right heart (anterior view).

FIGURE 5. A physiological and unusual pattern of MIBG uptake (Patient 16). Bilateral upper thoracic uptake with low thyroid uptake leading to a linear appearance (anterior view).
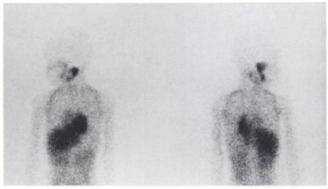
FIGURE 6. A physiological and unusual pattern of MIBG uptake (Patient 12). Pleural uptake is clearly detectable around the lungs on both anterior (left) and posterior (right) views.

faint, can be seen due to uptake of free iodine. An unequivocal normal scan is presented in Figure 1.

RESULTS

Difficulties in interpreting the scans were observed at the level of the thorax (15 patients), the abdomen (5 patients), the head (4 patients) or elsewhere (4 patients). The definitive interpretation of the scans was attributed to an age-dependent physiological pattern (10 patients), tumoral context (16 patients) or artifacts (2 patients).

Normal Pattern: Unusual Particularities in Children

The myocardial uptake is very intense in children less than 6 mo old (Fig. 2) and a particularly heterogeneous aspect of the right paramedian mediastinal image could lead to misinterpretation (Fig. 3). Another, previously undescribed pattern of MIBG uptake is an upper thoracic, symmetrical, linear, arciform and moderate physiological uptake (Patients 21 and 23). This phenomenon can be very intense, especially in younger patients (Figs. 4 and 5). This upper thoracic sign may be due to a curiously localized pleural uptake which rarely extends to the entire pleura (Fig. 6).
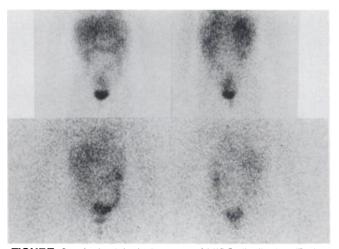

FIGURE 8. A physiological pattern of MIBG distribution (Patient 6). Intense colonic uptake on anterior (left) and posterior (right) views. Twenty-four hours after intravenous injection of MIBG (top), a retroperitoneal recurrence may be suspected; 48 hr later (bottom), distribution and intensity of the physiological digestive uptake have changed. No retroperitoneal recurrence is detectable on the four images.

Superimposition of bone and physiological areas of uptake, such as salivary glands, can be misleading; uptake in the salivary glands can be intense (Patient 14) and the presence of radioactive saliva in the mouth should be an indication to repeat the image projection (Fig. 7). The photopenic area in the gastric region in babies after a meal (Fig. 1) is easily recognized. The colonic depiction is generally easily recognized on delayed images since the intensity or topography may vary (Fig. 8).

Interpretative Difficulties Related to the Tumoral Context

Retrocardiac focus due to a posterior costal metastasis (Fig. 9) must be differentiated from very intense physiological myocardial uptake. A sharply delineated focus of uptake at the level of the right heart is abnormal and may be
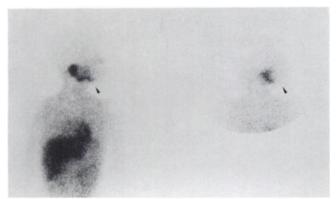

FIGURE 7. A physiological pitfall (Patient 12) with irregular wavy uptake at the level of the mandible (left) is not typical of a bony metastasis. No abnormal uptake is detectable at the same site when imaged a few minutes later (right).

FIGURE 9. A pitfall related to the tumoral context (Patient 1). On the anterior projection (left), the intensity of the myocardial uptake is unusually intense for a 2.5-yr-old patient. On posterior view (right), the cardiac shape is irregular. Radiology (CT) diagnosed a retrocardiac costal tumor. A frontal metastasis is seen on both projections.
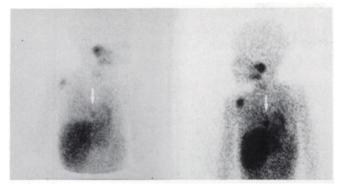
806

FIGURE 10. A pitfall related to the tumoral context (Patient 10). During the follow-up of a 5-yr-old girl known to be in complete remission of a stage IV neuroblastoma (left), the anterior thoracic view shows a scapular recurrence and an abnormal paramedian mediastinal uptake at the level of the right heart. One month later (right), the sternal metastasis can be easily recognized on the same view.

FIGURE 12. A pitfall related to the tumoral context (Patient 7). On anterior (left) and posterior (right) views, the upper thoracic sign cannot be physiological because it is unilateral with a high intensity and a heterogeneous appearance. Radiology diagnosed a supraclavicular tumoral lymph node. The right adrenal primary tumor is clearly depicted. The site of an enormous necrotic epigastric metastasis could not be scintigraphically identified. Radiology (US, CT) diagnosed left liver involvement.

related to a sternal metastasis (Fig. 10), a retroventricular vertebral metastasis (Patient 8) or an artifact of injection through a central catheter (Fig. 11). A relatively photopenic heart which has been previously reported in pheochromocytoma (12), is frequently observed in patients bearing neuroblastoma tumor sites (Patients 15 and 22).

A scapular or a costal skeletal metastasis or a supraclavicular lymph node (Fig. 12) should be differentiated from the physiological upper thoracic uptake. Pulmonary metastases concentrating MIBG may be visible (Fig. 13) and this must be differentiated from physiological lung uptake of tracer.

Only metastases with intense MIBG uptake, heterogeneous aspect or massive liver tumoral involvement (Fig. 12) will be distinguished from physiological liver uptake. In such cases, it is difficult to distinguish left liver uptake from splenic uptake (Patient 5). An intravenous injection of
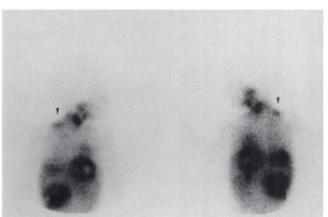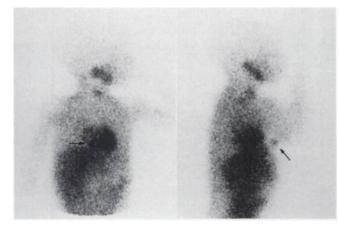
^{99m}Tc-colloid is helpful in delineating the limits of the MIBG liver uptake (Patient 20).

Pelvic bones are always difficult to identify on normal scans because they are superimposed on significant abdominal and muscular background. Equivocal areas of uptake in front of iliac bones generally resolve on later images (Patient 8). On posterior views, normal photopenic appearance of the spine interrupted by abnormal uptake is generally a sign of a vertebral metastasis, but it could also be related to abdominal lymph node involvement or residual tumor (Patient 17). Negative scintigraphic findings at the site of bone pain can be correlated with metastases which do not concentrate MIBG as demonstrated by subsequent ^{99m}Tc-HMDP bone scintigraphy (Patient 11).

FIGURE 11. An artifact of injection (Patient 9). On anterior view (left), a focus of pseudo-uptake is detectable at the level of the right ventricular MIBG uptake. On a profile view (right), the pseudo-lesion lies outside the thorax and the stasis of tracer in the central catheter by which MIBG was injected is confirmed.

FIGURE 13. An unusual tumoral aspect (Patient 1). Intense pulmonary uptake related to multiple interstitial pulmonary metastases (anterior view). Liver and bony metastases (humerus, rachis) are also detected. The myocardial uptake of MIBG is particularly low.
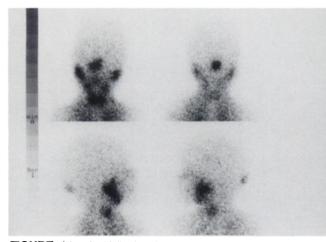
FIGURE 14. A pitfall related to the tumoral context (Patient 2), of a child known to be in complete remission of a Stage IV-S neuroblastoma. On anterior views (top, left), the nasal mucosal uptake is unusually intense and is not symmetrical. On posterior view (top, right) the intensity of the pseudo-nasal uptake is greater than on the anterior view. Lateral views (bottom) show an abnormal focus of occipital uptake which persists after hair washing. A biopsy was performed only on the basis of scintigraphic findings and after skin marking confirmed the recurrence of neuroblastoma.

The normal nasal musocal uptake should not be more intense on posterior than on anterior projections. If so, an occipital bone metastasis should be suspected (Fig. 14).

One particular problem is presented by Stage IV-S neuroblastoma with multiple subcutaneous metastases which render the exclusion of underlying bone involvement diffi-
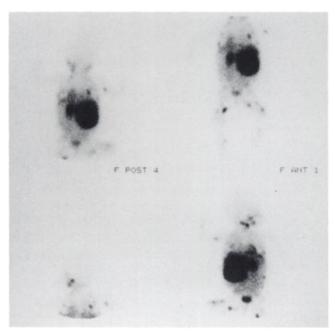

FIGURE 15. An unusual tumoral aspect (Patient 3). Stage IV-S neuroblastoma as demonstrated by the liver infiltrated with tumor and multiple subcutaneous metastases. The normal bony appearance cannot be clearly discerned.

cult (Fig. 15). A rare cervical primary tumor is easily distinguished (Patient 18) from a physiological uptake site. After cervical surgery and radiotherapy, a hemicranial photopenic focus can be observed (Patient 18).

Artifacts

A hand-injection artifact is easily identified (Patient 4). A more baffling pitfall originates from tracer stasis in a thoracic central catheter, resulting in an irregular appearance of myocardial uptake (Fig. 11).

DISCUSSION

Normal patterns of MIBG scintigraphy in children give rise to numerous particularities. Only follow-up allowed us to validate these patterns as physiological uptake. The unusual upper thoracic activity has never been described before. This appearance may be attributed to pleural uptake; no specific evidence other than appearance confirms the location of this uptake, nevertheless, it is well matched with the upper area of pleural uptake and occasionally extends to the entire pleura (Fig. 6).

The large number of physiological areas of uptake in soft tissues can lead to false-positive interpretations of normal scans, which can be avoided by attention to detail (Table 3). Careful nursing avoids urinary contamination. Repeat and delayed imaging generally rule out frequent gastrointestinal or urinary pitfalls. If necessary, intravenous injection of furosemide can eliminate tracer stasis in the urinary tract. In some cases, repeat imaging with high-activity ^{123}I-MIBG and SPECT helps to distinguish tumor sites from foci of physiological uptake.

Repeated views can also eliminate the pseudomandibulary uptake due to the presence of radioactive saliva in the mouth. This phenomenon can be seen even though neuronal MIBG uptake by the salivary glands is known to prevail over the local active glandular accumulation of free iodine. In some cases, an isolated focus of bony uptake may call for biopsy because of its prognostic importance. We have never observed the presence of normal positive MIBG uptake by the bones in a child. The normal MIBG image of the bones is free of uptake and any significant bony uptake indicates an osteomedullary invasion by a tumor concentrating MIBG. This is a major advantage over ^{99m}Tc-diphosphonate bone scans in neuroblastoma (13–15).

The most difficult problem remains the interpretation of normal adrenal gland MIBG uptake after unilateral adrenalectomy; size and intensity of uptake of the remaining contralateral gland may increase. This normal postsurgical reaction is difficult to distinguish from a retroperitoneal recurrence. Not even the most highly experienced observer can be aware of all interpretative difficulties of post-surgical adrenal patterns, especially in tumors known to be potentially bilateral (16,17). In such cases, only correlative images or clinical follow-up will lead to the correct diagnosis.

False-negative results are very rare if positive tumoral MIBG uptake was present at initial diagnosis (11) and may

TABLE 3
Causes, Frequency and Solutions to Avoid False-Positive and False-Negative Interpretation of MIBG Scans in Children

Causes	Frequency of false-positive studies	Frequency of false-negative studies	Solutions
Urinary contamination	+++	+	Nursing care (change clothing and wash patient prior to imaging)
Digestive uptake	++++	++++	Repeated and delayed imaging
Adrenal glands	+++	++	Experience
Urinary tract and bladder	+++	++	Delayed images Lateral projections ^{99m}Tc-DTPA-furosemide
Hepatic images	+	++++	^{99m}Tc-colloid
Thyroid uptake	++	+	Lugol's solution Lateral views
Upper thoracic uptake	+++		Experience
Myocardial uptake	+	++	Lateral views
Salivary glands or excretion	+	+	Repeated and delayed imaging Four cranial views
Nasal mucosa	+		Four cranial views
Pulmonary	+		Experience
Squelettical muscles	+		SPECT
Artifact of injection	++	+	Context and follow-up

Frequency of equivocal scans: + = rare; ++ = low frequency; +++ = often seen; and ++++ = common.

be expected, especially in heavily pretreated patients (this probably results from changes in the metabolic activity of the tumor and its foci of recurrence or metastases late in the course of the disease). According to our experience, this is seldom an indication for a ^{99m}Tc-HMDP bone scan.

Every unusual area of uptake on an MIBG scan in a child should be carefully analyzed. When not clearly correlated to a physiological or pathological pattern, further investigation by imaging modalities other than scintigraphy or, depending on the clinical consequences, follow-up by means of serial MIBG scans may be warranted.

Frequency of equivocal scans depends on the physician's experience; we believe it would be helpful to present our experience for improved interpretation of these problem cases (Table 3).

CONCLUSION

MIBG scintigraphy is well established as a major imaging modality in pediatric oncology providing high sensitivity and specificity in neuroblastoma. Nevertheless, the number of false-positive and false-negative interpretations should be minimized by drawing on a detailed knowledge of the unusual appearance of the variations of the normal scintigraphic pattern, including a precise interpretative analysis which will avoid numerous potential pitfalls.

ACKNOWLEDGMENTS

The authors thank the technical staff and nurses of the nuclear medicine and pediatric departments for their assistance and Ingrid Kuchenthal for reviewing this manuscript and Brahm Shapiro for helpful discussion.

REFERENCES

1. Wieland DM, Wu J, Brown LE, Manger TJ, Swanson DP, Beierwaltes WH. Radiolabeled adrenergic neuron-blocking agents: adrenomedullary imaging with ^{131}I-meta-iodobenzylguanidine. *J Nucl Med* 1980;21:349-353.
2. Manger TJ, Wu JL, Wieland DM. Solid phase exchange radioiodination of aryl iodide facilitation by ammonium sulfate. *J Org Chem* 1982;47:1484-1488.
3. Nakajo M, Shapiro B, Copp J, et al. The normal and abnormal distribution of the adrenomedullary imaging agent m-(^{131}I) iodobenzylguanidine (^{131}I-MIBG) in man: evaluation by scintigraphy. *J Nucl Med* 1983;24:672-682.
4. Shapiro B, Copp JE, Sisson JC, Eyre PL, Wallis J, Beierwaltes WH. Iodine-131-metaiodobenzylguanidine for the locating of suspected pheochromocytoma: experience in 400 cases. *J Nucl Med* 1985;26:576-585.
5. Treuner J. Use of ^{131}I-metaiodobenzylguanidine in pediatric oncology. *Nuklearmedizin* 1985;24:26-28.
6. Voute PA, Hoefnagel CA, Marcuse HR, de Kraker J. Detection of neuroblastoma with ^{131}I-metaiodobenzylguanidine. *Prog Clin Biol Res* 1985;175:389-398.
7. Hoefnagel CA, Voute PA, de Kraker J, Marcuse HR. Total-body scintigraphy with ^{131}I-metaiodobenzylguanidine for detection of neuroblastoma. *Diag Imag Clin Med* 1985;54:21-27.
8. Kimming B, Brandeis WE, Eisenhut M, et al. Scintigraphy of a neuroblastoma with ^{131}I-metaiodobenzylguanidine. *J Nucl Med* 1984;25:773-775.
9. Munker T. Iodine-131-metaiodobenzylguanidine scintigraphy of neuroblastomas. *Semin Nucl Med* 1985;15:154-160.
10. Lumbroso J, Hartmann O, Lemerle J, et al. Scintigraphic detection of neuroblastoma using ^{131}I and ^{123}I-labeled metaiodobenzylguanidine [Abstract]. *Eur J Nucl Med* 1985;11:A16.
11. Lumbroso J, Guermazi F, Hartman O, et al. Metaiodobenzylguanidine (MIBG) scans in neuroblastoma: sensitivity and specificity, a review of 115 scans. *Prog Clin Biol Res* 1988;271:689-705.
12. Nakajo M, Shapiro B, Glowniak J, Sisson JC, Beierwaltes WH. Inverse relationship between cardiac accumulation of meta-[^{131}I]iodobenzyl guanidine (^{131}I-MIBG) and circulating catecholamines in suspected pheochromocytoma. *J Nucl Med* 1983;24:1127-1134.
13. Heisel MA, Miller JH, Reid BS, Siegel SE. Radionuclide bone scan in neuroblastoma. *Pediatrics* 1983;71:206-209.
14. Howman-Giles RB, Gilday DL, Eng B, Ash JM. Radionuclide skeletal survey in neuroblastoma. *Radiology* 1979;131:497-502.
15. Kaufman RA, Thrall JH, Keyes JW, Brown ML, Zakem JF. False-negative

bone scans in neuroblastoma metastatic to the end of the long bones. *Am J Roentgenol* 1978;130:131–135.

16. D'Angio GJ. Neuroblastoma overview. *Med Pediatr Oncol* 1986;15:159–162.

17. Voute PA, de Kraker, Burgers JMV. Tumors of sympathetic nervous system: neuroblastoma, ganglioneuroma and pheochromocytoma. In: Voute PA, Barret A, Bloom HJG. Neidhardt MK, eds. *Cancer in children: clinical management, 2nd edition*. Berlin: Springer Verlag; 1985:238–251.

Condensed from
30 Years Ago:

Early Diagnosis of Metastatic Bone Cancer by Photoscanning with Strontium-85

N. David Charkes and David M. Sklaroff

Department of Radiology, Albert Einstein Medical Center, Northern Division, Philadelphia, Pennsylvania

This report describes the use of the ^{85}Sr photoscan to detect bones metastases in 90 patients with proven cancer and with suspected or demonstrable bone metastases. In many instances, as confirmed by bone biopsy, the scan revealed areas of tumor-laden bone, although roentgenograms of the same parts were interpreted as normal.

Strontium-85 was obtained from Oak Ridge in the form of the nitrate, with a specific activity of 2720 mCi/g or greater. Purity was greater than 90%, with less than 1% ^{89}Sr. Strontium-85 has a half-life of 64 days and decays by electron capture to ^{85}Rb, emitting a single gamma photon of 0.513 MeV in the process. There is no associated particulate emission, and the internal conversion coefficient is less than 1%. As a result, the radiation dose to bone from a 50-μCi dose is primarily from the gamma photons in bone. This dose was calculated to be approximately 0.80 rads, and the whole-body dose 0.34 rads.

A Picker Magnascanner was used exclusively for these studies. This instrument is equipped with a 3 x 2-inch sodium iodide (TA) crystal, 19-hole focusing collimator and a pulse-height analyzer.

Display is both on Teledeltos paper and on clear x-ray film (photoscan). It is more convenient to read the photoscan, but both read-out methods are employed for diagnosis.

Photoscans of bone utilizing 50 μCi of ^{85}Sr were obtained from 90 patients with cancer, with proven or suspected metastases to bone. In 11 patients, the scan was positive and the x-ray negative; in 75 other patients there was good agreement between the scan and the roentgenogram. The scan, however, frequently showed greater involvement than was apparent on x-ray. These results were confirmed by bone biopsy in 14 patients. Phantom studies were carried out which indicated that there is good correlation between the scan and known isotopic volumes within bone. Bone tissue counts of radiostrontium content were also correlated with biopsy findings, lending further support to the validity of the method.

It is therefore clear that the ^{85}Sr photoscan can detect early metastatic cancer to bone prior to observable roentgenographic changes. Not only have these scans been of value in diagnosis, but they have allowed the radiation therapist to plan treatment portals more effectively.